

## Cancer-promoting role of adipocytes in asbestos-induced mesothelial carcinogenesis through dysregulated adipocytokine production

Shan Hwu Chew<sup>1</sup>, Yasumasa Okazaki<sup>1</sup>,  
Hirotaka Nagai<sup>1,2</sup>, Nobuaki Misawa<sup>1</sup>, Shinya Akatsuka<sup>1</sup>,  
Kyoko Yamashita<sup>1</sup>, Li Jiang<sup>1</sup>, Yoriko Yamashita<sup>1</sup>,  
Michio Noguchi<sup>3</sup>, Kiminori Hosoda<sup>3,4</sup>, Yoshitaka Sekido<sup>5</sup>,  
Takashi Takahashi<sup>6</sup> and Shinya Toyokuni<sup>1,\*</sup>

<sup>1</sup>Department of Pathology and Biological Responses, Nagoya University Graduate School of Medicine, Nagoya 466-8550, Japan, <sup>2</sup>Department of Pathology and Biology of Diseases, <sup>3</sup>Department of Endocrinology and Metabolism and <sup>4</sup>Faculty of Human Health Science, Kyoto University Graduate School of Medicine, Kyoto 606-8315, Japan, <sup>5</sup>Division of Molecular Oncology, Aichi Cancer Center Research Institute, Nagoya 464-8681, Japan and <sup>6</sup>Department of Molecular Carcinogenesis, Nagoya University Graduate School of Medicine, Nagoya 466-8550, Japan

\*To whom correspondence should be addressed. Tel: +81 52 744 2086;  
Fax: +81 52 744 2091;  
Email: [toyokuni@med.nagoya-u.ac.jp](mailto:toyokuni@med.nagoya-u.ac.jp)

**Like many other human cancers, the development of malignant mesothelioma is closely associated with a chronic inflammatory condition. Both macrophages and mesothelial cells play crucial roles in the inflammatory response caused by asbestos exposure. Here, we show that adipocytes can also contribute to asbestos-induced inflammation through dysregulated adipocytokine production. 3T3-L1 preadipocytes were differentiated into mature adipocytes prior to use. These cells took up asbestos fibers (chrysotile, crocidolite and amosite) but were more resistant to asbestos-induced injury than macrophages and mesothelial cells. Expression microarray analysis followed by reverse transcription-PCR revealed that adipocytes respond directly to asbestos exposure with an increased production of proinflammatory adipocytokines [e.g. monocyte chemoattractant protein-1 (MCP-1)], whereas the production of anti-inflammatory adipocytokines (e.g. adiponectin) is suppressed. This was confirmed in epididymal fat pad of mice after intraperitoneal injection of asbestos fibers. Such dysregulated adipocytokine production favors the establishment of a proinflammatory environment. Furthermore, MCP-1 marginally promoted the growth of MeT-5A mesothelial cells and significantly enhanced the wound healing of Y-MESO-8A and Y-MESO-8D human mesothelioma cells. Our results suggest that increased levels of adipocytokines, such as MCP-1, can potentially contribute to the promotion of mesothelial carcinogenesis through the enhanced recruitment of inflammatory cells as well as a direct growth and migration stimulatory effect on mesothelial and mesothelioma cells. Taken together, our findings support a potential cancer-promoting role of adipocytes in asbestos-induced mesothelial carcinogenesis.**

### Introduction

Malignant mesothelioma, which arises from the mesothelial cells lining the pleural, peritoneal and pericardial cavity, is closely associated with exposure to asbestos fibers. The first convincing evidence of an etiologic relationship between asbestos fibers and malignant mesothelioma emerged in 1960 (1). Since then, there has been

**Abbreviations:** Ccl, chemokine C-C motif ligand; FBS, fetal bovine serum; IL-6, interleukin-6; MCP-1, monocyte chemoattractant protein-1; mRNA, messenger RNA; MTT, thiazolyl blue tetrazolium bromide; NT-tngl, tangled carbon nanotubes; PAI-1, plasminogen activator inhibitor-1; Prl2c5, prolactin family 2, subfamily c, member 5; RT-PCR, reverse transcription-PCR.

considerable interest in unraveling the mechanisms underlying asbestos-induced mesothelial carcinogenesis. Macrophages were the first to receive great attention, as asbestos exposure is often associated with a chronic granulomatous inflammatory response. Several groups reported the activation of macrophages by asbestos fibers, and they showed that asbestos fibers were able to induce macrophages to release a multitude of factors, such as lysosomal enzymes, cytokines, plasminogen activators and reactive oxygen species (2–4), which collectively contribute to chronic inflammation. Subsequent studies revealed a direct interaction between asbestos fibers and mesothelial cells, and asbestos fibers were shown to be able to activate certain signaling cascades within mesothelial cells. This activation might be critical for mesothelial transformation (5–8). In addition, mesothelial cells themselves also play a role in the inflammatory response. Mesothelial cells are particularly sensitive to the cytotoxic effect of asbestos fibers. Yang *et al.* (9) termed the process of asbestos-induced mesothelial cell death as ‘programmed necrosis’, and they reported that during this process, there was an extensive release of high-mobility group box 1 into the extracellular space, which then initiated a chronic inflammatory response by inducing the macrophages to release tumor necrosis factor- $\alpha$ . Together, this evidence strongly supports the vital role of chronic inflammation in asbestos carcinogenicity.

To establish an animal model of mesothelioma, asbestos fibers are usually injected into the pleural or peritoneal cavity (10–12). According to some previous reports, the peritoneal cavity appeared to be more sensitive to the effect of asbestos fibers compared with the pleural cavity, i.e. malignant mesothelioma developed more frequently and rapidly in the peritoneal cavity following asbestos injection (13,14). We speculated that this finding might be related to the abundance of adipose tissue in the peritoneal cavity. A substantial body of recent evidence has revealed the role of adipose tissue in inflammation, particularly in obesity-related inflammation (15–17). This inflammatory response in the adipose tissue of obese individuals is linked to the development of type 2 diabetes mellitus.

Adipose tissue is now recognized as an endocrine organ that is capable of secreting a wide variety of biologically active peptides collectively known as adipocytokines [e.g. monocyte chemoattractant protein-1 (MCP-1), interleukin-6 (IL-6), leptin, adiponectin, plasminogen activator inhibitor-1 (PAI-1), resistin and visfatin]. Evidence from numerous epidemiologic studies has revealed an increased risk of cancer development in obese individuals, further supporting a cancer-promoting role of adipose tissue (18–21). Obesity has been defined as a low-grade chronic inflammatory condition. Many groups have reported that the dysregulated endocrine function of adipose tissue underlies this obesity-related inflammation (22–25). Dysregulation of adipose tissue generally results in the enhanced production of pro-inflammatory adipocytokines and suppression of anti-inflammatory adipocytokines.

Some previous studies have demonstrated the ability of adipocytes to perform phagocytosis in a macrophage-like manner (26,27). A direct interaction between asbestos fibers and adipocytes involving fiber internalization is thus very likely to take place. We hypothesized that this interaction can trigger off an inflammatory response in adipocytes which occurs through dysregulation of adipocytokine production, as in obesity. Due to the close anatomic proximity between adipocytes and mesothelial cells, altered levels of adipocytokines can potentially affect mesothelial cells in a paracrine manner. We performed this study to evaluate the potential involvement of adipose tissue as a cancer promoter in asbestos-induced carcinogenesis through its ability to aggravate the inflammatory response.

## Materials and methods

### Materials

Three types of Union for International Cancer Control asbestos fibers (chrysotile A, crocidolite and amosite) were suspended in physiological saline. Tangled carbon nanotubes (NT-tngl, diameter = 15 nm; VGCF-X, Showa Denko, Tokyo, Japan) were suspended in physiological saline containing 0.5% bovine serum albumin. The 3T3-L1 preadipocyte cell line was a kind gift from Dr M.N. and Prof. K.H. (Kyoto University, Kyoto, Japan). MeT-5A and RAW264.7 cell lines were obtained from American Type Culture Collection (Manassas, VA). Y-MESO-8A and Y-MESO-8D cell lines were kindly provided by Prof. Y.S. (Aichi Cancer Centre Research Institute, Nagoya, Japan). These two human mesothelioma cell lines were established from the same Japanese patient with biphasic-like characteristics of malignant pleural mesothelioma and they showed epithelial and sarcomatous phenotypes, respectively, in cell culture (28). Recombinant human MCP-1 was purchased from PeproTech (Rocky Hill, NJ). Thiazolyl blue tetrazolium bromide (MTT) was purchased from Sigma (St Louis, MO). Dimethyl sulfoxide was purchased from Wako (Osaka, Japan).

### Cell culture

3T3-L1 preadipocytes were maintained in Dulbecco's modified Eagle's medium supplemented with 10% calf serum and antibiotics. The differentiation of these preadipocytes into mature adipocytes was induced with Dulbecco's modified Eagle's medium supplemented with 10% fetal bovine serum (FBS), 0.5 mM 3-isobutyl-1-methyl-xanthine, 0.25  $\mu$ M dexamethasone and 1  $\mu$ g/ml insulin. Mature adipocytes were used for experiments within 10–14 days after the induction of differentiation. The RAW264.7 macrophage cell line was maintained in Dulbecco's modified Eagle's medium supplemented with 10% FBS and antibiotics. MeT-5A, a human mesothelial cell line immortalized through transfection with the pRSV-T plasmid (an SV40 ori-construct containing the SV40 early region and the Rous sarcoma virus long terminal repeat), was maintained in M199 medium supplemented with 10% FBS, 10 ng/ml epidermal growth factor, 870 nM insulin, 400 nM hydrocortisone, 0.3% (vol/vol) trace element B and antibiotics. Y-MESO-8A and Y-MESO-8D cell lines were maintained in RPMI 1640 medium supplemented with 10% FBS and antibiotics. All the cells were cultured in a humidified incubator with 5% CO<sub>2</sub> at 37°C.

### Experimental animals

For animal experiments, 8-week-old male ddY mice (Japan SLC, Hamamatsu, Shizuoka, Japan) were used. The animals were housed in a specific pathogen-free animal facility with 12h light/12h dark cycle and allowed free access to food (CE-2, CLEA Japan, Tokyo, Japan) and water. These mice were subjected to a single intraperitoneal injection of 2.5 mg of asbestos fibers and killed after 3 days via cervical dislocation. Physiological saline (0.9%) was injected as a control. After killing, the epididymal fat pad was harvested; half of it was fixed in 10% phosphate-buffered formalin for histological analysis, whereas the other half was snap-frozen in liquid nitrogen and kept at -80°C until further use. The animal experiment was approved by the Animal Experiment Committee of the Nagoya University Graduate School of Medicine.

### Oil Red O staining of adipocytes

Adipocyte maturation from the preadipocyte cell line was confirmed by staining the lipid droplets that accumulated in the cytoplasm of adipocytes during maturation using the Oil Red O staining method. After washing the mature adipocytes with phosphate-buffered saline, the cells were fixed with 10% phosphate-buffered formalin for 2 h. After another washing step, Oil Red O solution was added, and the cells were incubated at 37°C for 5 min. Images were acquired using a Nikon Eclipse TS-100 microscope (Nikon, Tokyo, Japan).

### Fiber uptake by adipocytes

The uptake of asbestos fibers by adipocytes was analyzed by both light microscopy and transmission electron microscopy. Cultured adipocytes were exposed to 10  $\mu$ g/cm<sup>2</sup> of asbestos fibers, and 24 h later, the cells were harvested by trypsinization and centrifuged to generate a cell pellet. For light microscopy, cell block was prepared by fixing the cells with 10% phosphate-buffered formalin and subsequently processed into a paraffin-embedded cell block. Sections of 4  $\mu$ m were stained with Kernechtrot staining and viewed under  $\times$ 100 magnification using a BZ-9000 microscope (Keyence, Osaka, Japan) to detect fibers inside the cells. For electron microscopy, cells were fixed with phosphate buffer containing 2.5% glutaraldehyde and 2% paraformaldehyde, followed by fixation with 1% osmium tetroxide. The cells were then embedded in Epon resin and cut into 80 nm ultrathin sections with diamond knife. After staining with uranyl acetate and lead citrate, detection of fibers inside the cells was performed using JEM-1400EX transmission electron microscope (JEOL, Tokyo, Japan).

### Cell viability assay

The cytotoxicity of asbestos fibers on adipocytes, MeT-5A and RAW264.7 macrophages was measured using a CellTiter-Glo Luminescent Cell Viability Assay (Promega, Madison, WI). Asbestos fibers were added to the cells at a concentration of 10  $\mu$ g/cm<sup>2</sup>. After 72 h of incubation, the number of viable cells was evaluated via the addition of the CellTiter-Glo Luminescent Cell Viability Assay reagent followed by chemiluminescence measurement using a PowerScan4 plate reader (DS Pharma Biomedical, Osaka, Japan).

### Microarray-based gene expression analysis

Microarray analysis was performed using an Agilent SurePrint G3 Mouse GE 8x60K Microarray slide and Agilent's Low Input Quick Amp Labeling Kit (Agilent Technologies, Santa Clara, CA) according to Agilent's One-Color Microarray-Based Gene Expression Analysis protocol. In total, 200 ng of total RNA extracted from adipocytes exposed to asbestos fibers under the conditions stated above was used as the initial material. Amplified cRNA was labeled with Cy3-CTP. Hybridization was performed by placing the slide in a hybridization oven equipped with a rotator and set at 65°C for 17 h. After hybridization, the microarray slide was washed with GE Wash Buffer and scanned, and data were analyzed using GeneSpring GX 10.02.2 software (Agilent Technologies).

### Quantitative real-time reverse transcription-PCR

Total RNA was isolated from the differentiated adipocyte cell line or adipose tissue using the RNeasy Lipid Tissue Mini Kit (Qiagen, Valencia, CA). Total RNA was then reverse transcribed into complementary DNA using the SuperScript III First-Strand Synthesis Kit (Invitrogen, Grand Island, NY). Gene expression levels were quantitatively measured using the Platinum SYBR Green qPCR SuperMix-UDG kit (Invitrogen) and analyzed with an Applied Biosystems Model 7300 Real Time PCR System (Applied Biosystems, Foster City, CA). The  $\beta$ -actin level was used to normalize the messenger RNA (mRNA) level of all genes examined. The primer sequences used were as follows: mouse IL-6, forward, 5'-CTTCTGGGACTGATGCTGG-3', reverse, 5'-CAGAATTGCCATTGCACAAC-3' (product size 185 bp); mouse  $\beta$ -actin, forward, 5'-ACATCCCCAAAGTTCTACAAA-3', reverse, 5'-TGAGGGACTTCCTGTAACCACT-3' (product size 132 bp); mouse adiponectin, forward, 5'-GCAGGCATCCCAGGACATCC-3', reverse, 5'-TCCTTTCTGCCAGGGGTTTC-3' (product size 186 bp); mouse MCP-1, forward, 5'-CAGTTAACGCCCACTCCAC-3', reverse, 5'-TCCTCTTGGGGTCAAGCA-3' (product size 163 bp); mouse prolactin family 2, subfamily c, member 5 (Prl2c5), forward, 5'-AACAGGAACAAGCCAGGCACA-3', reverse, 5'-ACCCCGTTCTGGACTGCGTT-3' (product size 188 bp); mouse leptin, forward, 5'-CCAGCTGCAAGGTGCAAGA-3', reverse, 5'-CCCTCTGCTTGGCGGATACCGA-3' (product size 214 bp) and mouse PAI-1, forward, 5'-ATGTGCACCTCTCCGCCCTCA-3', reverse, 5'-GCTGCTCTTGGTCGGAAAGACTTG-3' (product size 213 bp).

### MCP-1 enzyme-linked immunosorbent assay

Differentiated adipocytes in a 6-well plate were exposed to different types of asbestos fibers and NT-tngl at 10  $\mu$ g/cm<sup>2</sup> for 72 h. The cell culture medium was then collected, and the concentration of MCP-1 secreted by adipocytes into the culture medium was measured using the Quantikine Mouse JE/MCP-1 Immunoassay Kit (R&D Systems, Minneapolis, MN). The immunoassay was performed according to the manufacturer's instructions.

### Immunohistochemistry

Paraffin-embedded tissue sections were deparaffinized and rehydrated. Antigen retrieval was performed by heating the sections with microwave using 10 mM citrate buffer, pH 6.0. Endogenous peroxidase was inhibited by incubating the sections with 0.3% hydrogen peroxide in methanol for 30 min. Tissue sections were then blocked with normal goat serum and incubated with rabbit polyclonal primary antibody against mouse MCP-1 (ab7202, abcam, Tokyo, Japan) or IL-6 (ab6672; abcam). After washing with phosphate-buffered saline, sections were incubated with biotinylated goat anti-rabbit immunoglobulin G secondary antibody. Detection of antigen-antibody complexes was performed by incubating the sections with horseradish peroxidase-conjugated streptavidin followed by 3,3'-diaminobenzidine. Images were acquired using BZ 9000 microscope.

### Measurement of adipocyte size

Images of epididymal adipose tissue sections were acquired using BZ 9000 microscope at  $\times$ 40 magnification. Ten random fields were taken for each section from five animals per group. Cell surface area was measured using ImageJ software (NIH, Bethesda, MD).

### Transwell migration assay

Cell culture inserts and 24-well companion tissue culture plates from BD Falcon (Franklin Lakes, NJ) were used for transwell migration assay. The

cell culture insert contains a porous membrane with an 8  $\mu\text{m}$  pore size. RAW264.7 macrophages were seeded into the insert at a density of  $2 \times 10^5$  cells/insert. Conditioned medium collected from adipocytes that were treated or untreated with asbestos fibers was added to the lower chamber of the 24-well tissue culture plate. The plate was incubated for 24 h, followed by staining of the migrated cells with May–Grunwald's and Giemsa stains. Images were acquired in 10 random fields, and the number of migrated cells was counted.

#### MTT cell proliferation assay

MeT-5A cells were seeded into a 96-well tissue culture plate at a density of  $5 \times 10^3$  cells/well. These cells were serum starved for 24 h before being treated with recombinant human MCP-1 at a concentration of 100 and 500 ng/ml. After 72 h of treatment, cell proliferation was measured using MTT. The MTT compound was dissolved in phosphate-buffered saline at a concentration of 5 mg/ml, and 20  $\mu\text{l}$  was then added to each well. Cells were incubated with MTT for 4 h to allow the reduction of MTT into purple formazan. Culture

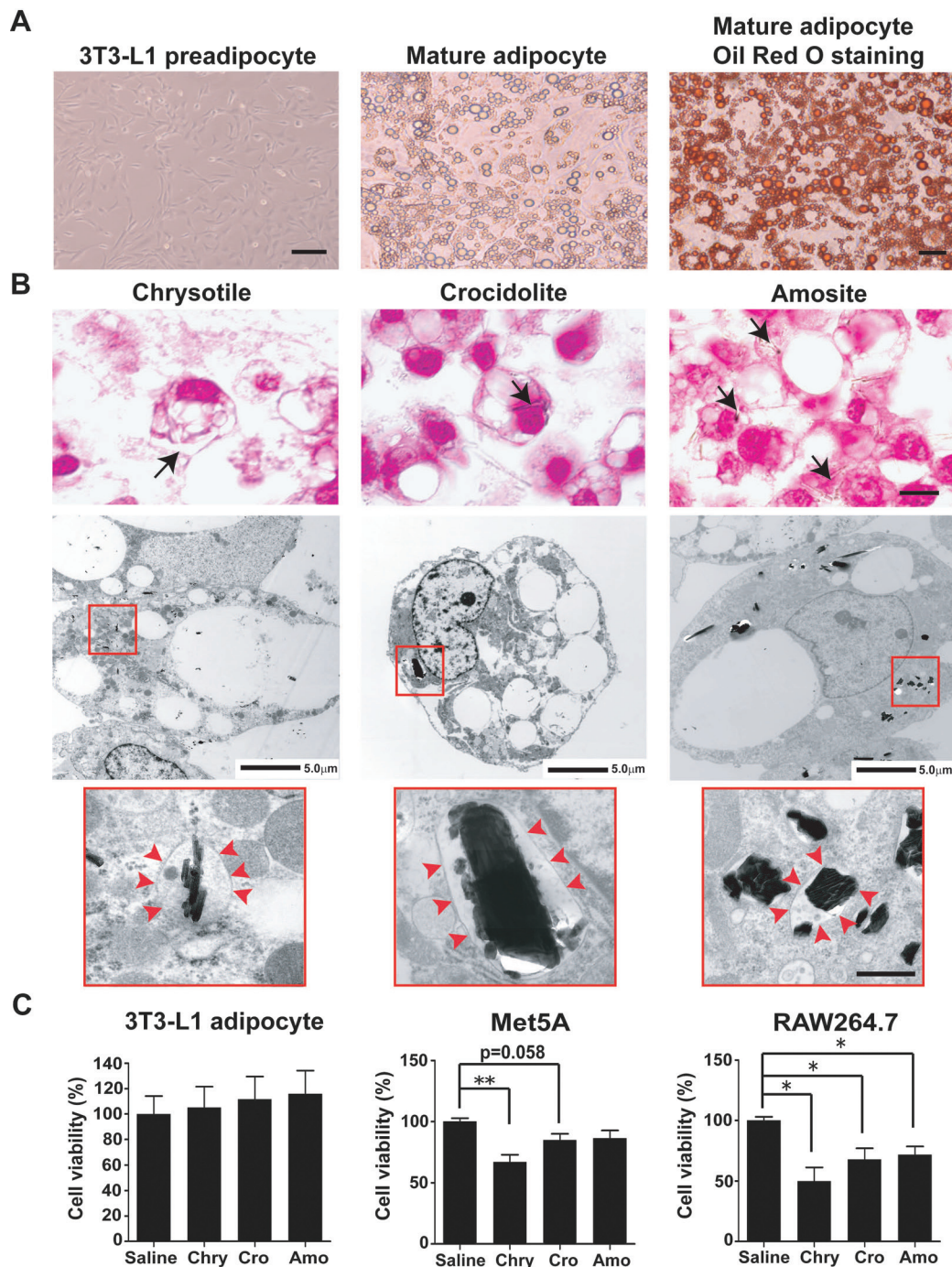


**Fig. 1.** Cultured adipocytes take up asbestos fibers but are resistant to their cytotoxic effect. (A) The 3T3-L1 preadipocyte cell line (left panel) was differentiated into mature adipocytes (middle panel) according to the standard differentiation protocol. Lipid droplets that accumulated in the mature adipocytes were stained by Oil Red O staining (right panel). Scale bars: left panel, 100  $\mu\text{m}$ ; middle and right panels, 20  $\mu\text{m}$ . (B) The presence of asbestos fibers inside adipocytes was detected using light microscopy at  $\times 100$  magnification (upper panel) and transmission electron microscopy (middle and lower panels). Scale bars: upper panel, 10  $\mu\text{m}$ ; middle panel, 5  $\mu\text{m}$ ; lower panel, 500 nm. (C) The cytotoxicity of asbestos fibers on adipocytes, MeT-5A mesothelial cells and RAW264.7 macrophages was measured by the adenosine triphosphate cell viability assay. All the cells were exposed to 10  $\mu\text{g}/\text{cm}^2$  of asbestos fibers for 72 h. The results are shown as the mean  $\pm$  SEM of three independent experiments. \* $P \leq 0.05$ , \*\* $P \leq 0.005$ . Amo, amosite; Chry, chrysotile; Cro, crocidolite.

medium containing MTT was then aspirated from the wells, followed by the addition of 100 µl of dimethyl sulfoxide into each well to dissolve the purple formazan crystals. The optical density was measured using a PowerScan4 plate reader.

#### Wound-healing assay

MeT-5A, Y-MESO-8A or Y-MESO-8D cells were grown in a 6-well tissue culture plate until the cells formed a confluent monolayer. A scratch was then made across the cell monolayer using a pipette tip. Recombinant human MCP-1 was added to some of the wells at a concentration of 500 ng/ml.

Images of the wound were taken immediately after the scratch (designated as 0h) and at 18, 24 and 48h after the scratch. The width of the wound was measured using ImageJ software, and the percentage of wound healing was then calculated.

#### Statistical analysis

The statistical significance between two groups of interest was analyzed using the unpaired Student's *t*-test. A *P* value of <0.05 was considered significant.

**Table I.** Top 20 genes upregulated in asbestos-treated cultured adipocytes

Gene name	Accession number	Fold change
Top 20 genes upregulated in chrysotile-treated adipocytes		
Prolactin family 2, subfamily c, member 5 (Prl2c5)	NM_181852	18.596165
Fibrinogen-like protein-1 (Fgl1)	BC029734	8.48526
Chemokine (C-C motif) ligand 2 (Ccl2)	NM_011333	8.051252
Troponin T2, cardiac (Tnnt2), transcript variant 9	NM_011619	6.9297132
Prolactin family 2, subfamily c, member 1 (Prl2c1)	NM_001045532	6.292936
Secreted phosphoprotein 1 (Spp1)	NM_009263	5.334665
High-mobility group AT-hook 2 (Hmga2)	NM_010441	5.1633744
Chemokine (C-C motif) ligand 8 (Ccl8)	NM_021443	4.867768
lincRNA:chr19:9060613-9060851 forward strand		4.497705
Fos-like antigen 1 (Fosl1)	NM_010235	4.422233
Interleukin 1 receptor-like 1 (Il1rl1), transcript variant 1	NM_001025602	4.192457
Tumor necrosis factor receptor superfamily, member 9 (Tnfrsf9), transcript variant 1	NM_011612	4.0868807
Plasminogen activator, urokinase (Plau)	NM_008873	4.038391
Runt-related transcription factor 1 (Runx1), transcript variant 2	NM_001111022	3.8444314
Interleukin 1 receptor-like 1 (Il1rl1), transcript variant 2	NM_010743	3.7691207
cDNA sequence BC023744 (BC023744)	NM_001033311	3.6094844
Matrix metalloproteinase 10 (Mmp10)	NM_019471	3.6034727
Matrix metalloproteinase 13 (Mmp13)	NM_008607	3.5614529
Serine/threonine/tyrosine kinase 1 (Styk1)	NM_172891	3.4867864
Acyl-CoA synthetase bubblegum family member 1 (Acsbg1)	NM_053178	3.3379452
Top 20 genes upregulated in crocidolite-treated adipocytes		
Serum amyloid A 3 (Saa3)	NM_011315	21.692352
Haptoglobin (Hp)	NM_017370	11.54753
Dermokine (Dmkn), transcript variant 3	NM_001166173	9.095255
Suprabasin (Sbsn), transcript variant 1	NM_172205	7.677543
Secretory leukocyte peptidase inhibitor (Slpi)	NM_011414	6.6974707
Serine (or cysteine) peptidase inhibitor, clade A, member 3G (Serpina3g)	NM_009251	6.258521
PREDICTED: <i>Mus musculus</i> predicted gene, EG628900 (EG628900)	XM_893705	6.231637
Chemokine (C-C motif) ligand 2 (Ccl2)	NM_011333	5.961754
Chemokine (C-C motif) ligand 9 (Ccl9)	NM_011338	5.94364
Chitinase 3-like 1 (Chi3l1)	NM_007695	5.8167386
Lipocalin-2 (Lcn2)	NM_008491	5.732993
Chemokine (C-X-C motif) receptor 7 (Cxcr7)	NM_007722	5.6649795
Prolactin family 2, subfamily c, member 5 (Prl2c5)	NM_181852	5.511816
Complement component 4B (Childo blood group) (C4b)	NM_009780	5.504423
Serine (or cysteine) peptidase inhibitor, clade A, member 3H (Serpina3h)	NM_001034870	5.3198853
Runt-related transcription factor 1 (Runx1), transcript variant 4	NM_009821	5.090166
Triggering receptor expressed on myeloid cells 2 (Trem2)	NM_031254	4.8963866
Fibrinogen-like protein 1 (Fgl1)	NM_145594	4.8214192
Cannabinoid receptor 1 (brain) (Cnr1)	NM_007726	4.818088
Placental protein 11 related (Pp11r), transcript variant 2	NM_001168693	4.759451
Top 12 genes upregulated in amosite-treated adipocytes		
Extended synaptotagmin-like protein 3 (Esyt3)	NM_177775	2.988655
Budding uninhibited by benzimidazoles 1 homolog ( <i>Saccharomyces cerevisiae</i> ) (Bub1)	NM_009772	2.4976056
Potassium inwardly rectifying channel, subfamily J, member 6 (Kcnj6)	NM_001025585	2.4706264
lincRNA:chr4:21683562-21694344 reverse strand		2.4663801
PREDICTED: <i>M. musculus</i> predicted gene, EG666955 (EG666955)	XM_001000153	2.3627758
lincRNA:chr2:75493715-75494227 reverse strand		2.3625197
Adult male tongue cDNA, RIKEN full-length enriched library, clone:2310006M14	AK009188	2.271196
product:hypothetical protein, full insert sequence		
ATPase, Ca <sup>++</sup> transporting, type 2C, member 2 (Atp2c2)	NM_026922	2.2707396
lincRNA:chr6:31017987-31174287 reverse strand		2.2265513
Adult male olfactory brain cDNA, RIKEN full-length enriched library, clone:6430601O08	AK032580	2.2096734
product:similar to Pol protein (fragment) ( <i>M. musculus</i> ), full insert sequence		
lincRNA:chr19:59498190-59531390 reverse strand		2.1915858
lincRNA:chr17:27479404-27481770 forward strand		2.082444

ATPase, adenosine triphosphatase; cDNA, complementary DNA. Twelve genes with >2-fold change were selected for amosite.

## Results

### Uptake of asbestos fibers by cultured adipocytes

The 3T3-L1 preadipocyte cell line was used to generate mature adipocytes according to the standard differentiation protocol. Adipocytes were used for subsequent experiments 10–14 days after the initiation of differentiation. During differentiation, the adipocytes accumulated lipid droplets in the cytoplasm that stained red upon Oil Red O staining (Figure 1A). Three different types of asbestos fibers, chrysotile, crocidolite and amosite fibers, were added to the adipocytes, followed by the assessment of fiber uptake using a cell block and light microscopy. Fiber uptake by the adipocytes was observed for all the asbestos types (Figure 1B, upper panel). Our findings were further supported by transmission electron microscopy, which clearly demonstrated fiber internalization by adipocytes (Figure 1B, lower panel). High magnification revealed the structure of a vesicular membrane around the asbestos fibers.

Asbestos fibers induce cell death when administered to mesothelial cells and macrophages (7,29). We compared the cytotoxicity of asbestos fibers on the cultured adipocytes, MeT-5A mesothelial cells and RAW264.7 macrophages by exposing them to the same concentration of asbestos fibers ( $10 \mu\text{g}/\text{cm}^2$ ). When we performed an adenosine triphosphate detection cell viability assay on these different cell types, we did not observe any cytotoxic effect of asbestos fibers on the adipocytes, which was in contrast to mesothelial cells and macrophages (Figure 1C).

### Cultured adipocytes showed changes in gene expression after asbestos exposure

As noted above, we hypothesized that the endocrine function of adipose tissue is potentially affected by asbestos exposure. To screen for genes with altered expression in asbestos-exposed adipocytes, we performed microarray gene expression analysis on the total RNA isolated from adipocytes after 72 h of exposure to asbestos fibers (GEO accession no.: GSE42330). The microarray results are shown in Table I. The top 20 genes that were upregulated in adipocytes after exposure to the different types of asbestos fibers are listed. More information can be found in the Supplementary Tables 1–3, available at *Carcinogenesis* Online. Gene expression analysis revealed the upregulation of some inflammation-related genes in adipocytes following exposure to asbestos fibers, including serum amyloid A3, haptoglobin and urokinase-type plasminogen activator. More importantly, we found the upregulation of an important adipocytokine that is commonly reported to be upregulated in obesity and is responsible for the related chronic inflammation and associated metabolic complications: chemokine C-C motif ligand 2 (Ccl2), which is also known as MCP-1. Other members of the C-C motif chemokine family were also upregulated, such as Ccl6, Ccl8 and Ccl9. Another gene that was upregulated in both chrysotile- and crocidolite-treated adipocytes was Prl2c5, which belongs to the prolactin superfamily.

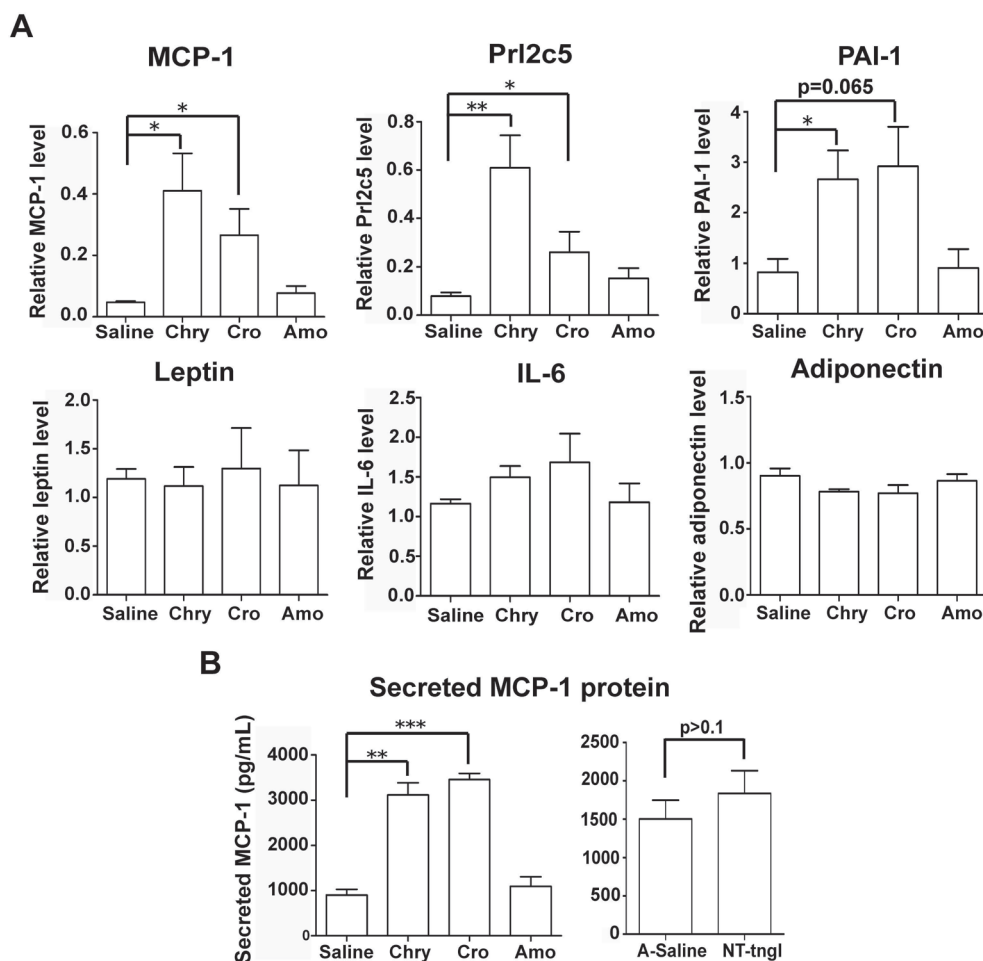


**Fig. 2.** Alterations in the expression level of adipocytokines in cultured adipocytes after asbestos exposure. Cultured adipocytes were exposed to chrysotile, crocidolite or amosite fibers at  $10 \mu\text{g}/\text{cm}^2$  for 72 h, with physiological saline as the control. (A) The gene expression level of various adipocytokines was measured by quantitative real-time RT-PCR and is shown relative to that of  $\beta$ -actin. (B) The secretion of MCP-1 into culture medium was measured by an MCP-1 immunoassay. In addition to asbestos fibers, adipocytes were also exposed to NT-tngl under the same experimental condition. The results are shown as the mean  $\pm$  SEM of three independent experiments, \* $P \leq 0.05$ , \*\* $P \leq 0.005$ , \*\*\* $P \leq 0.001$ . Amo, amosite; A-Saline, saline containing 0.5% bovine serum albumin; Chry, chrysotile; Cro, crocidolite.

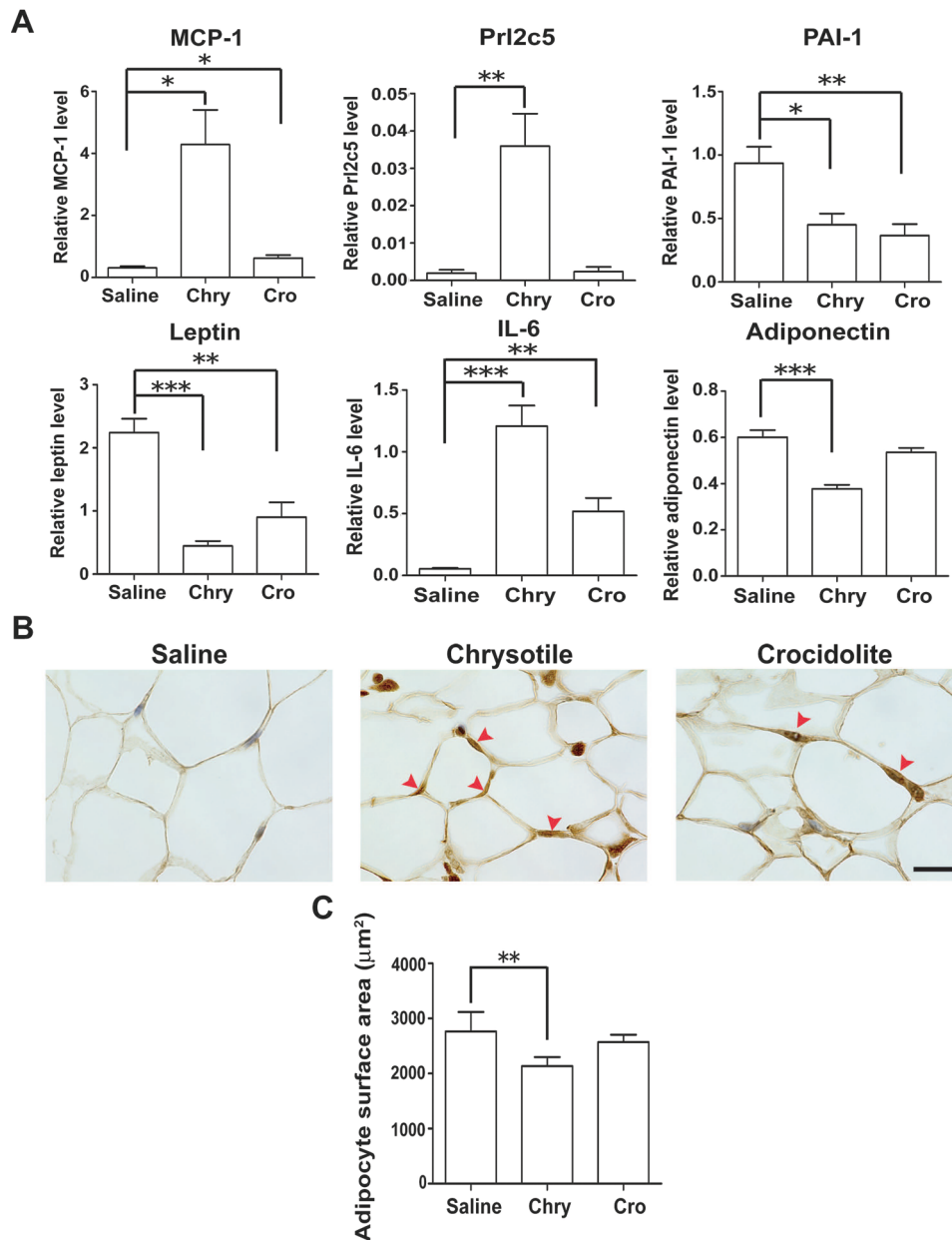


**Fig. 3.** Adipose tissues of mice injected with asbestos fibers show changes in adipocytokine expression levels. A total of 2.5 mg of chrysotile or crocidolite fibers was injected into the peritoneal cavity of mice, with physiological saline used as a control. Epididymal adipose tissue was harvested after 3 days. (A) The gene expression level of various adipocytokines in the epididymal adipose tissue was measured by quantitative real-time RT-PCR. The results are shown as the mean  $\pm$  SEM ( $n = 6$  per group). (B) Representative images of epididymal adipose tissue immunostained for MCP-1 expression. Scale bar: 20  $\mu$ m. (C) Measurement of adipocyte cell surface area from adipose tissue sections using image analyzing software ( $n = 5$  per group). \* $P \leq 0.05$ , \*\* $P \leq 0.005$ , \*\*\* $P \leq 0.001$ . Chry, chrysotile; Cro, crocidolite.

#### MCP-1 was increased at the mRNA and protein level in adipocytes treated with asbestos fibers

Quantitative real-time reverse transcription-PCR (RT-PCR) was performed to evaluate the expression level of MCP-1, Prl2c5 and several other commonly known adipocytokines (PAI-1, leptin, IL-6 and adiponectin) in asbestos-treated or untreated adipocytes. In support of the microarray results, quantitative real-time RT-PCR showed the increased mRNA expression of MCP-1 and Prl2c5 in adipocytes following asbestos exposure (Figure 2A). Regarding the other adipocytokines examined, PAI-1 was also upregulated, whereas leptin, IL-6 and adiponectin did not show any significant alterations. Nevertheless, a slight decrease in adiponectin mRNA expression was observed. An enzyme-linked immunosorbent assay was performed

to measure the secretion of MCP-1 protein into the culture medium of adipocytes treated with asbestos fibers. The enzyme-linked immunosorbent assay results corroborated those of quantitative real-time RT-PCR, showing a significant elevation of MCP-1 secretion by adipocytes treated with chrysotile and crocidolite fibers (control = 900.7 pg/ml, chrysotile treated = 3116.5 pg/ml, crocidolite treated = 3455.9 pg/ml,  $P \leq 0.005$ ) (Figure 2B, left panel). Amosite-treated adipocytes did not show any apparent change in MCP-1 expression at either the mRNA or protein level. To determine whether any type of particulate is able to induce the same response, we also exposed the adipocytes to NT-tngl. Exposure to NT-tngl did not induce any significant increase in MCP-1 secretion from the adipocytes (Figure 2B, right panel).

### Asbestos fibers dysregulated adipocytokine levels in adipose tissue of asbestos-exposed mice

To determine whether adipose tissue in living animals also responds to asbestos exposure, we injected chrysotile or crocidolite fibers into the peritoneal cavity of mice, with physiological saline as a control. Epididymal fat pads were harvested after 3 days, followed by quantitative real-time RT-PCR to examine changes in the expression level of adipocytokines. Again, the mRNA levels of MCP-1 and Prl2c5 were both upregulated in the adipose tissue of mice injected with asbestos fibers (Figure 3A). Regarding adiponectin, its suppressed expression level in the adipose tissue was more apparent than in the cultured adipocytes and was significant in chrysotile-injected mice. Leptin and IL-6 were significantly downregulated and upregulated, respectively, although no significant change in these two genes was observed in cultured adipocytes (Figure 2A). PAI-1 was the only exception that showed contradictory results between *in vitro* and *in vivo* assays. Immunohistochemical staining for MCP-1 and IL-6 was also performed on the adipose tissue sections. We found that in both chrysotile and crocidolite-injected mice, there was more intense MCP-1 staining in the cytoplasm of adipocytes compared with the saline-injected mice (Figure 3B). In contrast, the adipocytes did not show apparent positive staining of IL-6 (Supplementary Figure 1, available at *Carcinogenesis* Online), indicating that other inflammatory cells might be responsible for IL-6 mRNA upregulation as shown in Figure 3A. We have also noted some changes in adipocyte size and measurement of adipocyte surface area revealed a reduction of adipocyte size in asbestos-injected mice (Figure 3C).

### MCP-1 promoted cancer cell phenotypes of mesothelial cells

Based on the well-known effect of MCP-1 as a macrophage chemoattractant, the increased secretion of MCP-1 by adipocytes in response to asbestos fibers might implicate an important indirect role of adipose tissue in enhancing the recruitment of macrophages to the sites of asbestos deposition. We collected culture media from asbestos-treated adipocytes and examined the ability of these conditioned media to induce macrophage migration. The transwell migration assay results revealed an increase in macrophage migration in response to the conditioned media from asbestos-treated adipocytes, which was most probably mediated by increased MCP-1 secretion (Figure 4).

Many chemokines have been reported to exert a mitogenic effect and are thus able to promote cancer development. We studied the effect of MCP-1 on mesothelial cell proliferation by treating MeT-5A cells with recombinant MCP-1 protein. MCP-1 showed a marginal but not significant effect on mesothelial cell proliferation (Figure 5A). In addition, we assayed the effect of MCP-1 on mesothelial cell migration. A wound-healing assay was performed in MeT-5A cells in the presence or absence of recombinant MCP-1 protein. We did not observe any effect of MCP-1 on MeT-5A cell migration (Figure 5B, left panel). However, we found that MCP-1 promoted the migration of the human mesothelioma cells Y-MESO-8A and Y-MESO-8D (Figure 5B, middle and right panels).

### Discussion

Our results revealed for the first time that asbestos fibers are able to directly affect the endocrine activity of adipocytes. This effect might be mediated through a direct interaction, as we showed that adipocytes were able to phagocytose asbestos fibers. Although adipose tissue is more abundant in the peritoneal cavity, it is also present in the pleural cavity, e.g. submesothelial space of the parietal pleura, around the pericardial sac and near the mediastinum (30,31). These anatomic locations render relevance of adipose tissue as it is accessible for the inhaled fibers through fiber translocation. In response to asbestos exposure, adipocytes upregulated proinflammatory adipocytokine such as MCP-1 but suppressed the level of anti-inflammatory

## Macrophage migration

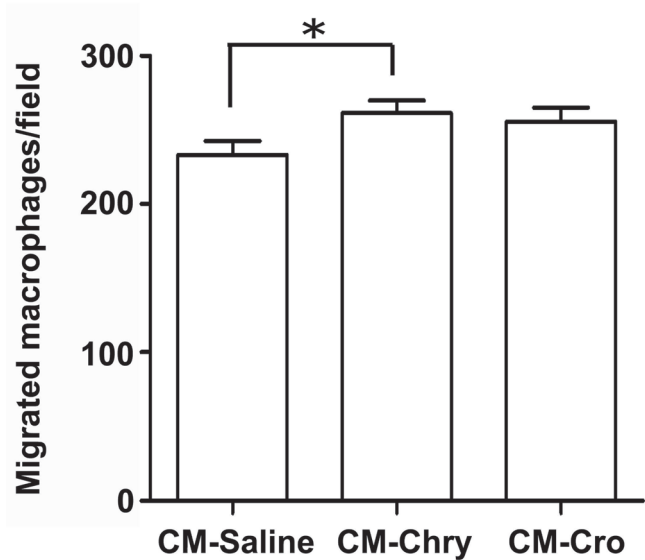


**Fig. 4.** Adipocytes induce increased macrophage migration following asbestos exposure. Cultured adipocytes were exposed to chrysotile or crocidolite fibers at 10  $\mu\text{g}/\text{cm}^2$  for 72 h, with physiological saline as a control. Conditioned medium was collected and assayed with a transwell migration assay to determine the ability of the conditioned media to induce macrophage migration. The results are shown as the mean  $\pm$  SEM of three independent experiments. \* $P \leq 0.05$ . Chry, chrysotile; CM, conditioned medium; Cro, crocidolite.

adipocytokine, adiponectin, thereby shifting the balance towards a proinflammatory condition. Increased MCP-1 secretion by adipocytes might result in enhanced macrophage recruitment which in turn elaborates various cytokines and chemokines, leading to a vicious cycle that aggravates inflammation. Our results using adipocyte conditioned media to induce macrophage migration supported this notion. The role of adipose tissue in asbestos-induced inflammation can thus be both direct and indirect. MCP-1 has been reported to induce the proliferation of primary human pleural mesothelial cells (32) and our results using MeT-5A are consistent with the report. We also showed that MCP-1 promoted the migration of human mesothelioma cells. In addition, we observed a reduction in adipocyte size in asbestos-injected mice, which is probably due to the more active state of the adipocytes that requires higher metabolic rate.

MCP-1 transgenic and MCP-1<sup>-/-</sup> mice have previously been generated and characterized. MCP-1 overexpression in specific organs resulted in the enhanced recruitment of blood monocytes into the parenchyma of these organs (33,34). In contrast, in MCP-1<sup>-/-</sup> mice, there is a reduction in mononuclear cell infiltrate when these mice are challenged with different inflammatory stimuli (35). These mouse models are often used in studies related to obesity and insulin resistance. Kanda *et al.* (24) generated adipose-specific MCP-1 transgenic mice characterized by insulin resistance, hepatic steatosis and a higher degree of macrophage infiltration into adipose tissue. These MCP-1 genetically engineered mice might be a useful tool in our further studies to establish an association between MCP-1 expression and asbestos-induced mesotheliomagenesis.

In this study, we primarily focused on the possible tumor-promoting effects of MCP-1. Other adipocytokines with dysregulated expression might also play a cancer-promoting role. For instance, adiponectin expression is inversely correlated with human cancers. Low circulating levels of adiponectin have been associated with an increased risk of several cancers, such as colorectal cancer (36), endometrial cancer (37), postmenopausal breast cancer (38), gastric cancer (39) and prostate cancer (40). Adiponectin was reported to be able to inhibit the transcription factor nuclear factor- $\kappa\text{B}$  (41,42), which is

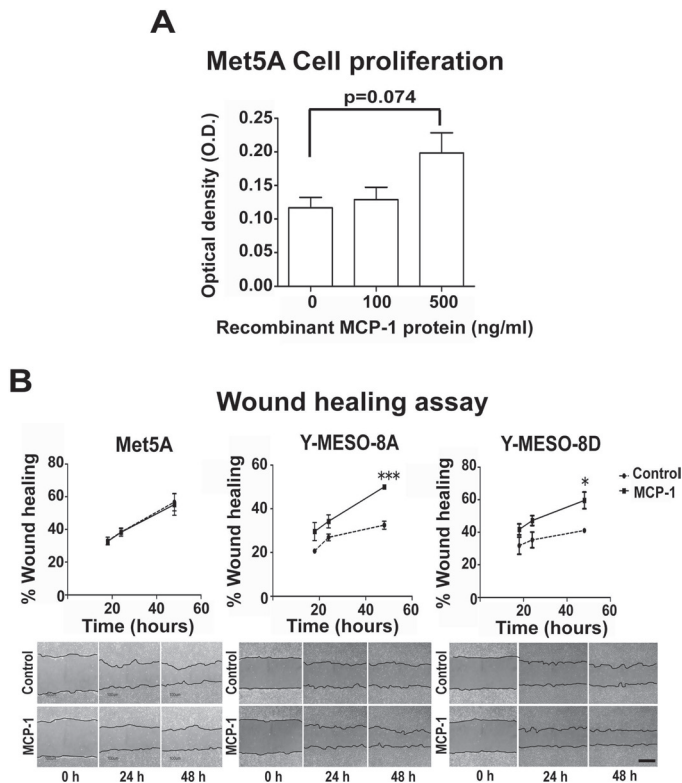


**Fig. 5.** Cancer-promoting effects of MCP-1. (A) Recombinant MCP-1 protein stimulates cell proliferation of the human mesothelial cell line MeT-5A, as measured by the MTT cell proliferation assay. (B) Recombinant MCP-1 protein induces the migration of the human mesothelioma cells Y-MESO-8A and Y-MESO-8D, as measured by the wound-healing assay. The results are shown as the mean  $\pm$  SEM of three independent experiments. \* $P \leq 0.05$ , \*\*\* $P \leq 0.001$ .

a key molecule activated by asbestos fibers in mesothelial cells and macrophages that is responsible for inflammation. Our results suggested that asbestos fibers can cause a downregulation of adiponectin. The exact roles of leptin and PAI-1 in inflammation are still not entirely clear, although both were shown to be upregulated in obesity-related inflammation (43–45). A member of the prolactin superfamily, Prl2c5, was also upregulated. Current information regarding Prl2c5 is still relatively scarce, but this protein most probably shares many characteristics of prolactin, which is known to possess mitogenic property (46). Prolactin was newly found as an adipocytokine secreted by human adipose tissue (47,48). Several other genes more recently characterized as adipokines were also upregulated. Some of these genes, such as haptoglobin and lipocalin-2, bind to iron and can thus contribute to iron overload, which was shown to play an important role in asbestos-induced mesothelioma development (49). Another interesting upregulated peptide was secreted phosphoprotein 1, also known as osteopontin. Mesothelioma patients often have increased serum osteopontin levels and it was suggested to be a useful biomarker for the early diagnosis of mesothelioma (50). More detailed studies are needed to fully elucidate the potential pathogenic roles of these various dysregulated adipocytokines in mesothelial carcinogenesis. Moreover, a long-term study is needed to assess whether these alterations observed are long-term effects.

Interestingly, we found that chrysotile fibers appeared to be the most inflammogenic. Our results showed that chrysotile fibers dysregulated various adipocytokine levels to a higher extent than crocidolite and amosite fibers. This finding corroborates our recently published data that chrysotile fibers induced a significantly earlier development of malignant mesothelioma with intraperitoneal injection in rats compared with crocidolite and amosite fibers (49). The relatively stronger carcinogenicity of chrysotile fibers might be linked to a higher degree

of adipose tissue inflammation. The reason underlying why chrysotile fibers seem to have a stronger inflammogenic effect on adipocytes is still not known, although our results showed that all types of asbestos fibers were internalized by the adipocytes.

To our knowledge, this is the first report of a potential association between dysregulated adipose endocrine function and asbestos-induced mesothelial carcinogenesis. We have shown that asbestos fibers are able to directly trigger an inflammatory response in adipocytes by dysregulating adipocytokine production. These adipocytokines might act locally to stimulate the growth/migration/survival of mesothelial cells and thus promote the development of malignant mesothelioma. The modulation of these adipocytokines might represent a novel strategy to extend the lifespan of mesothelioma patients.

## Supplementary material

Supplementary Tables 1–3 and Figure 1 can be found at <http://carcin.oxfordjournals.org/>

## Funding

Princess Takamatsu Cancer Research Fund (10-24213); Ministry of Health, Labour and Welfare of Japan (25-A-5); Ministry of Education, Culture, Sports, Science and Technology of Japan (24390094). The funders had no role in study design, data collection and analysis, decision to publish or preparation of the manuscript.

*Conflict of Interest Statement:* None declared.

## References

- Wagner, J.C. *et al.* (1960) Diffuse pleural mesothelioma and asbestos exposure in the North Western Cape Province. *Br. J. Ind. Med.*, **17**, 260–271.
- Davies, P. *et al.* (1974) Asbestos induces selective release of lysosomal enzymes from mononuclear phagocytes. *Nature*, **251**, 423–425.
- Hamilton, J.A. (1980) Macrophage stimulation and the inflammatory response to asbestos. *Environ. Health Perspect.*, **34**, 69–74.
- Choe, N. *et al.* (1997) Pleural macrophage recruitment and activation in asbestos-induced pleural injury. *Environ. Health Perspect.*, **105** (suppl. 5), 1257–1260.
- Ramos-Nino, M.E. *et al.* (2002) Mesothelial cell transformation requires increased AP-1 binding activity and ERK-dependent Fra-1 expression. *Cancer Res.*, **62**, 6065–6069.
- Swain, W.A. *et al.* (2004) Activation of p38 MAP kinase by asbestos in rat mesothelial cells is mediated by oxidative stress. *Am. J. Physiol. Lung Cell. Mol. Physiol.*, **286**, L859–L865.
- Yang, H. *et al.* (2006) TNF- $\alpha$  inhibits asbestos-induced cytotoxicity via a NF- $\kappa$ B-dependent pathway, a possible mechanism for asbestos-induced oncogenesis. *Proc. Natl Acad. Sci. USA*, **103**, 10397–10402.
- Jagadeeswaran, R. *et al.* (2006) Functional analysis of c-Met/hepatocyte growth factor pathway in malignant pleural mesothelioma. *Cancer Res.*, **66**, 352–361.
- Yang, H. *et al.* (2010) Programmed necrosis induced by asbestos in human mesothelial cells causes high-mobility group box 1 protein release and resultant inflammation. *Proc. Natl Acad. Sci. USA*, **107**, 12611–12616.
- Whitaker, D. *et al.* (1984) Cytologic and tissue culture characteristics of asbestos-induced mesothelioma in rats. *Acta Cytol.*, **28**, 185–189.
- Suzuki, Y. *et al.* (1984) Malignant mesothelioma induced by asbestos and zeolite in the mouse peritoneal cavity. *Environ. Res.*, **35**, 277–292.
- Toyokuni, S. (2009) Mechanisms of asbestos-induced carcinogenesis. *Nagoya J. Med. Sci.*, **71**, 1–10.
- Bolton, R.E. *et al.* (1982) Variations in the carcinogenicity of mineral fibres. *Ann. Occup. Hyg.*, **26**, 569–582.
- Carthew, P. *et al.* (1992) Intrapleural administration of fibres induces mesothelioma in rats in the same relative order of hazard as occurs in man after exposure. *Hum. Exp. Toxicol.*, **11**, 530–534.
- Fantuzzi, G. (2005) Adipose tissue, adipokines, and inflammation. *J. Allergy Clin. Immunol.*, **115**, 911–9; quiz 920.
- Greenberg, A.S. *et al.* (2006) Obesity and the role of adipose tissue in inflammation and metabolism. *Am. J. Clin. Nutr.*, **83**, 461S–465S.
- Itoh, M. *et al.* (2011) Adipose tissue remodeling as homeostatic inflammation. *Int. J. Inflamm.*, **2011**, 720926.

18. Bianchini, F. *et al.* (2002) Overweight, obesity, and cancer risk. *Lancet Oncol.*, **3**, 565–574.
19. Calle, E.E. *et al.* (2003) Overweight, obesity, and mortality from cancer in a prospectively studied cohort of U.S. adults. *N. Engl. J. Med.*, **348**, 1625–1638.
20. Reeves, G.K. *et al.* Million Women Study Collaboration. (2007) Cancer incidence and mortality in relation to body mass index in the Million Women Study: cohort study. *BMJ*, **335**, 1134.
21. Renehan, A.G. *et al.* (2008) Body-mass index and incidence of cancer: a systematic review and meta-analysis of prospective observational studies. *Lancet*, **371**, 569–578.
22. Hotamisligil, G.S. *et al.* (1993) Adipose expression of tumor necrosis factor- $\alpha$ : direct role in obesity-linked insulin resistance. *Science*, **259**, 87–91.
23. Sartipy, P. *et al.* (2003) Monocyte chemoattractant protein 1 in obesity and insulin resistance. *Proc. Natl Acad. Sci. USA*, **100**, 7265–7270.
24. Kanda, H. *et al.* (2006) MCP-1 contributes to macrophage infiltration into adipose tissue, insulin resistance, and hepatic steatosis in obesity. *J. Clin. Invest.*, **116**, 1494–1505.
25. van Kruijsdijk, R.C. *et al.* (2009) Obesity and cancer: the role of dysfunctional adipose tissue. *Cancer Epidemiol. Biomarkers Prev.*, **18**, 2569–2578.
26. Cousin, B. *et al.* (1999) A role for preadipocytes as macrophage-like cells. *FASEB J.*, **13**, 305–312.
27. Villena, J.A. *et al.* (2001) Adipose tissues display differential phagocytic and microbicidal activities depending on their localization. *Int. J. Obes. Relat. Metab. Disord.*, **25**, 1275–1280.
28. Usami, N. *et al.* (2006) Establishment and characterization of four malignant pleural mesothelioma cell lines from Japanese patients. *Cancer Sci.*, **97**, 387–394.
29. Nagai, H. *et al.* (2011) Diameter and rigidity of multiwalled carbon nanotubes are critical factors in mesothelial injury and carcinogenesis. *Proc. Natl Acad. Sci. USA*, **108**, E1330–E1338.
30. Okby, N.T. *et al.* (2000) Liposarcoma of the pleural cavity: clinical and pathologic features of 4 cases with a review of the literature. *Arch. Pathol. Lab. Med.*, **124**, 699–703.
31. Shen, W. *et al.* (2003) Adipose tissue quantification by imaging methods: a proposed classification. *Obes. Res.*, **11**, 5–16.
32. Nasreen, N. *et al.* (2000) MCP-1 in pleural injury: CCR2 mediates haptotaxis of pleural mesothelial cells. *Am. J. Physiol. Lung Cell. Mol. Physiol.*, **278**, L591–L598.
33. Fuentes, M.E. *et al.* (1995) Controlled recruitment of monocytes and macrophages to specific organs through transgenic expression of monocyte chemoattractant protein-1. *J. Immunol.*, **155**, 5769–5776.
34. Gunn, M.D. *et al.* (1997) Monocyte chemoattractant protein-1 is sufficient for the chemotaxis of monocytes and lymphocytes in transgenic mice but requires an additional stimulus for inflammatory activation. *J. Immunol.*, **158**, 376–383.
35. Lu, B. *et al.* (1998) Abnormalities in monocyte recruitment and cytokine expression in monocyte chemoattractant protein 1-deficient mice. *J. Exp. Med.*, **187**, 601–608.
36. Wei, E.K. *et al.* (2005) Low plasma adiponectin levels and risk of colorectal cancer in men: a prospective study. *J. Natl Cancer Inst.*, **97**, 1688–1694.
37. Dal Maso, L. *et al.* (2004) Circulating adiponectin and endometrial cancer risk. *J. Clin. Endocrinol. Metab.*, **89**, 1160–1163.
38. Mantzoros, C. *et al.* (2004) Adiponectin and breast cancer risk. *J. Clin. Endocrinol. Metab.*, **89**, 1102–1107.
39. Ishikawa, M. *et al.* (2005) Plasma adiponectin and gastric cancer. *Clin. Cancer Res.*, **11** (2 Pt 1), 466–472.
40. Goktas, S. *et al.* (2005) Prostate cancer and adiponectin. *Urology*, **65**, 1168–1172.
41. Ajuwon, K.M. *et al.* (2005) Adiponectin inhibits LPS-induced NF- $\kappa$ B activation and IL-6 production and increases PPAR $\gamma$ 2 expression in adipocytes. *Am. J. Physiol. Regul. Integr. Comp. Physiol.*, **288**, R1220–R1225.
42. Wulster-Radcliffe, M.C. *et al.* (2004) Adiponectin differentially regulates cytokines in porcine macrophages. *Biochem. Biophys. Res. Commun.*, **316**, 924–929.
43. Auwerx, J. *et al.* (1988) Tissue-type plasminogen activator antigen and plasminogen activator inhibitor in diabetes mellitus. *Arteriosclerosis*, **8**, 68–72.
44. Juhan-Vague, I. *et al.* (1989) Increased plasminogen activator inhibitor activity in non insulin dependent diabetic patients—relationship with plasma insulin. *Thromb. Haemost.*, **61**, 370–373.
45. Hauner, H. (2005) Secretory factors from human adipose tissue and their functional role. *Proc. Nutr. Soc.*, **64**, 163–169.
46. Welsch, C.W. *et al.* (1977) Prolactin and murine mammary tumorigenesis: a review. *Cancer Res.*, **37**, 951–963.
47. Zinger, M. *et al.* (2003) Prolactin expression and secretion by human breast glandular and adipose tissue explants. *J. Clin. Endocrinol. Metab.*, **88**, 689–696.
48. Hugo, E.R. *et al.* (2008) Prolactin release by adipose explants, primary adipocytes, and LS14 adipocytes. *J. Clin. Endocrinol. Metab.*, **93**, 4006–4012.
49. Jiang, L. *et al.* (2012) Iron overload signature in chrysotile-induced malignant mesothelioma. *J. Pathol.*, **228**, 366–377.
50. Pass, H.I. *et al.* (2005) Asbestos exposure, pleural mesothelioma, and serum osteopontin levels. *N. Engl. J. Med.*, **353**, 1564–1573.

Received December 5, 2012; revised June 25, 2013; accepted July 31, 2013